

**One-dimensional Langevin models of fluid particle acceleration in developed turbulence**

A. K. Aringazin\* and M. I. Mazhitov†

*Department of Theoretical Physics, Institute for Basic Research, Eurasian National University, Astana 473021 Kazakhstan*

(Received 2 June 2003; revised manuscript received 20 October 2003; published 27 February 2004)

We make a comparative analysis of some recent one-dimensional Langevin models of the acceleration of a Lagrangian fluid particle in developed turbulent flow. The class of models characterized by random intensities of noises (RIN models) provides a fit to the recent experimental data on the acceleration statistics. We review the model by Laval, Dubrulle, and Nazarenko (LDN) formulated in terms of temporal velocity derivative in the rapid distortion theory approach, and propose its extension due to the RIN framework. The fit of the contribution to fourth-order moment of the acceleration is found to be better than in the other stochastic models. We study the acceleration probability density function conditional on velocity fluctuations implied by the RIN approach to the LDN-type model. The shapes of the conditional distributions and the conditional acceleration variance have been found in a good agreement with the recent experimental data by Mordant, Crawford, and Bodenschatz [Physica D (to be published), e-print physics/0303003].

DOI: 10.1103/PhysRevE.69.026305

PACS number(s): 47.27.Jv, 05.20.Jj

**I. INTRODUCTION**

Tsallis statistics [1] inspired formalism [2–4] was recently used by Beck [5,6] to describe Lagrangian statistical properties of developed turbulence; see also Refs. [7–9]. In recent papers [10–12] we have made some refinements of this approach. The probability density function of a component of the Lagrangian acceleration of infinitesimal fluid particle in the developed turbulent flow is found due to the equation

$$P(a) = \int_0^\infty d\beta P(a|\beta) f(\beta), \quad (1)$$

where  $P(a|\beta)$  is a conditional probability density function associated with a surrogate dynamical equation, the one-dimensional Langevin equation for the acceleration  $a$ ,

$$\partial_t a = \gamma F(a) + \sigma L(t). \quad (2)$$

Here,  $\partial_t$  denotes time derivative,  $F(a)$  is the deterministic drift force,  $\gamma$  is the drift coefficient,  $\sigma^2$  measures intensity of the noise, a strength of the additive stochastic force, and  $L(t)$  is Langevin source, a  $\delta$ -correlated Gaussian-white noise with zero mean,

$$\langle L(t) \rangle = 0, \quad \langle L(t)L(t') \rangle = 2\delta(t-t'), \quad (3)$$

where the averaging is made over ensemble realizations.

For constant parameters  $\gamma$  and  $\sigma$ , this usual Langevin model ensures that the stochastic process  $a(t)$  defined by Eq. (2) is Markovian. The probability density function  $P(a|\beta)$  of the acceleration at fixed  $\beta$ ,

$$\beta = \gamma/\sigma^2, \quad (4)$$

can be found as a stationary solution of the corresponding Fokker-Planck equation

$$\partial_t P(a,t) = \partial_a [-\gamma F(a) + \sigma^2 \partial_a] P(a,t), \quad (5)$$

where  $\partial_a = \partial/\partial a$ . This equation can be derived from the Langevin equation (2) using the noise (3) either in Stratonovich or Ito interpretations. Particularly, for a linear drift force  $F(a) = -a$ , the stationary probability density function  $\partial_t P(a,t) = 0$  is of a Gaussian form:

$$P(a|\beta) = C(\beta) \exp[-\beta a^2/2], \quad (6)$$

where  $C(\beta) = \sqrt{\beta/2\pi}$  is a normalization constant and  $a \in [-\infty, \infty]$ . The function  $f(\beta)$  entering Eq. (1) is a probability density function arising from the assumption that  $\beta$  is a random parameter with prescribed external statistics.

While it is evident that the three-dimensional Navier-Stokes equation with a  $\delta$ -correlated Gaussian-white random forcing belongs to a class of nonlinear stochastic dynamical equations for the velocity field with which one can associate some generalized Fokker-Planck equations, it is a theoretical challenge to make a link between the Navier-Stokes equation and surrogate one-dimensional Langevin models for acceleration such as Eq. (2). This model is, of course, far from being a full model of the essential Lagrangian dynamics of fluid in the developed turbulence regime.

Review and critical analysis of the applications of various recent nonextensive statistics based models to the turbulence have been made by Gotoh and Kraichnan [13]. An emphasis was made that some models lack justification of a fit from turbulence dynamics although being able to reproduce experimental data to more or less accuracy. A deductive support from the three-dimensional Navier-Stokes equation was stressed to be essential for the fitting procedure to be considered meaningful.

In contrast to the fluid particle velocity, the fluid particle acceleration

\*Also at Department of Mechanics and Mathematics, Kazakhstan Division, Moscow State University, Moscow 119899, Russia.  
Electronic address: aringazin@mail.kz

†Electronic address: mmi@emu.kz

$$a_i = \frac{dv_i}{dt} \equiv \partial_t v_i + v_k \partial_k v_i, \quad (7)$$

which incorporates the Eulerian local acceleration and nonlinear advection term, can be measured easier by using the Lagrangian framework while in the Eulerian framework (fixed probe) this requires measurements of the velocity  $v_i$  and temporal and spatial velocity derivatives  $\partial_t v_i$  and  $\partial_k v_i$ , where  $\partial_k = \partial/\partial x^k$  denotes spatial derivative in the Cartesian laboratory frame of reference;  $i, k = 1, 2, 3$ . In the Lagrangian framework, the Navier-Stokes equation can be written as

$$a_i = -\rho^{-1} \partial_i p + \nu \partial_k^2 v_i + f_i, \quad (8)$$

where  $\rho$  is constant fluid density,  $p$  is pressure,  $\nu$  is kinematic viscosity,  $v_i = \partial_t x_i$  is velocity, and  $f_i$  is forcing. Here,  $x_i = X_i(x_{0k}, t)$  is the particle coordinate viewed as a function of the initial value  $x_i(0) = x_{0i}$  and time  $t$  so that the measurement of time series  $x_i(t)$  of some individual particle by using a fine finite-difference scheme allows one to evaluate its acceleration as a function of time by using the Lagrangian relation

$$a_i = \partial_t^2 x_i. \quad (9)$$

With the initial data points  $x_{0i}$  (Lagrangian coordinates) running over all the fluid particles one gets a Lagrangian description of the fluid flow. Direct analytical evaluation of the acceleration from Eq. (8) is out of reach at present so that one is led to estimate it in some fashion.

The model (2) belongs to a class of stochastic models of Lagrangian turbulence and deals with an evolution of the acceleration in time which in accord to the Navier-Stokes equation is driven by time derivative on the right-hand side (rhs) of Eq. (8). This type of modeling corresponds to the well-known universality (Kolmogorov 1941, Heisenberg 1948, and Yaglom 1949) in statistically homogeneous and isotropic developed turbulence which is expected to occur in the inertial range only statistically. Accordingly, the velocity and acceleration become random, and one is interested in their probability density functions, or multipoint correlation functions. This is in an agreement with the observed temporally irregular character of the velocity and acceleration of a tracer particle in high-Reynolds-number turbulent flows. By the universality, statistics of the velocity and statistics of the acceleration do not depend on statistics of the forcing and chosen initial data. In this paper we are interested in statistics of one of the acceleration components,  $a$ , so that we model its evolution in time.

In a physical context, an essential fluid particle dynamics in the developed turbulent flow is described here in terms of a generalized Brownian-like motion, a stochastic particle approach, taking the particle acceleration (9) as the dynamical variable. Such models are generally based upon a hierarchy of characteristic time scales in the system and naturally employ one-point statistical description using Langevin-type equation (a stochastic differential equation of first order) for

the dynamical variable, or the associated Fokker-Planck equation (a partial differential equation) for one-point probability density function.

With the choice of  $\delta$ -correlated noises such models fall into the class of Markovian models (no memory effects at small scales) allowing well established Fokker-Planck approximation. The consideration of finite-time correlated noises and the associated memory effects requires a deeper analysis which should be made separately in each particular case. The evolution equations are formulated and solved in the Lagrangian framework (the comoving frame), in a purely temporal treatment, with fluctuations being treated along the particle trajectory.

Approximation of a short-time correlated noise by the zero-time correlated one is usually made due to the time-scale hierarchy emerging from the general physical analysis of the system and experimental data. Under the stationarity condition, a balance between the energy injected at large scales and the energy dissipated by viscous processes at small scales, one can try to solve the Fokker-Planck equation to find stationary probability density function of the acceleration,  $P(a)$ . This function as well as the associated moments can then be compared with the experimental data on acceleration statistics. The Fokker-Planck approximation allows one to make a link between the dynamics and the statistical approach. In the case when stationary probability distribution can be found exactly one can make a further analysis without a dynamical reference, yet having a possibility to extract stationary time correlators.

In contrast to the usual Brownian like motion, the fluid particle acceleration does not merely follow a random walk with a complete self-similarity at all scales. It was found to reveal a different, multiscale self-similarity, which can be seen from wide tails of a quasi-Gaussian distribution of the experimental probability distribution  $P(a)$ . This requires a consideration of some specific Langevin-type equations, which may include nonlinear terms, e.g., to account for turbulent viscosity effect, and an extension of the usual properties of model forces and additive and multiplicative noises.

Specifically, the class of models represented by Eqs. (1)–(6) is featured by consideration of the acceleration evolution driven by the “forces” characterized by fluctuating drift coefficient  $\gamma$  (or fluctuating intensity of multiplicative  $\delta$ -correlated noise in a more general case) and/or fluctuating intensity  $\sigma^2$  of the additive noise. This was found to imply stationary distributions of the acceleration (or velocity increments in time, for finite time lags) of a quasi-Gaussian form with wide tails which are a classical signature of the turbulence intermittency, a phenomenon which developed turbulent flows exhibiting at small time scales. Earlier work on such type of models are due to Castaing, Gagne, and Hopfinger [14], referred to as the Castaing model, in which a log-normal distribution of fluctuating variance of intermittent variable was used without reference to a stochastic dynamical equation.

The difference from the well-known class of stochastic models with  $\delta$ -correlated Gaussian-white multiplicative and additive noises which are also known to imply quasi-Gaussian stationary distributions with wide tails is that one

supposes that *intensities* of the noises are not constant but fluctuate at a large time scale. We refer to the models with such Random intensities of noises as RIN models.

This class of models introduces a two-time-scale dynamics, one associated with a  $\delta$  correlation of noises (modeling the smallest time scale under consideration, usually of the order of Kolmogorov time) and the other associated with variations of intensities of the noises, their possible coupling to each other, and other parameters assumed to occur at large time scales, up to a few Lagrangian integral times. From a general point of view, one can assume a hierarchy of a number of characteristic time scales. However, in the present paper we simplify the consideration in order to make it more analytically tractable, in accord to the presence of two characteristic time scales in the Kolmogorov picture of fully developed turbulence.

In the approximation of two time scales, one can start with a Langevin-type equation, derive the associated Fokker-Planck equation in Stratonovich or Ito formulations, and try to find a stationary solution of the Fokker-Planck equation, in which slowly fluctuating parameters are taken to be fixed. As the next step, one evaluates stochastic expectation of the resulting *conditional* probability density function over the parameters with some distributions assigned to them. By this way one can obtain a stationary marginal probability density function as the main prediction of the model.

The dynamical model (2) represents a particular simple one-dimensional RIN model characterized by the presence of an additive noise (a short time scale) and fluctuating composite parameter  $\beta = \gamma/\sigma^2$  (a long time scale), where  $\gamma$  is simply kinetic coefficient (a multiplicative noise is not present explicitly) and  $\sigma^2$  is the additive noise intensity.

Two-time-scale stochastic dynamics in describing the acceleration jointly with the velocity and position was used by Sawford [15]:

$$\begin{aligned} \partial_t a = & -(T_L^{-1} + t_\eta^{-1})a + T_L^{-1}t_\eta^{-1}u \\ & + \sqrt{2\sigma_u^2(T_L^{-1} + t_\eta^{-1})}T_L^{-1}t_\eta^{-1}L(t), \end{aligned} \quad (10)$$

$$\partial_t u = a, \quad \partial_t x = u, \quad (11)$$

where

$$T_L = \frac{2\sigma_u^2}{C_0\bar{\epsilon}}, \quad t_\eta = \frac{2a_0\nu^{1/2}}{C_0\bar{\epsilon}^{1/2}} \quad (12)$$

are two time scales,  $T_L \gg t_\eta$ ,  $C_0$ ,  $a_0$  are Lagrangian structure constants,  $\sigma_u^2$  is the variance of the velocity distribution, and  $\bar{\epsilon}$  is mean energy dissipation rate per unit mass. This model predicts Gaussian stationary distributions for the acceleration and velocity reflecting uncorrelated character of the fluctuations. An obvious extension of this model is to replace  $\bar{\epsilon}$  by stochastic energy dissipation rate  $\epsilon$ , and assume that it is log normally distributed in correspondence with the refined Kolmogorov 1962 approach [16].

Recently, an attempt to generalize the Sawford model to the case of fluctuating parameters has been made by Reynolds [9], with a good agreement with the experimental results being achieved.

The growing interest in studying Langevin-type equations to describe developed turbulence is motivated by the recent high precision Lagrangian experiments by Porta, Voth, Crawford, Alexander, and Bodenschatz [17], the new data by Crawford, Mordant, Bodenschatz, and Reynolds (the Taylor microscale Reynolds number is  $R_\lambda = 690$ , the normalized acceleration range is  $[-60, 60] \ni a$ , and the Kolmogorov time scale  $\tau_\eta$  is resolved) [18], Mordant, Delour, Leveque, Arneodo, and Pinton ( $R_\lambda = 740$ ,  $a \in [-20, 20]$ ,  $\tau_\eta$  is not resolved) [19], Mordant, Crawford, and Bodenschatz [20], and direct numerical simulations of the Navier-Stokes equation by Kraichnan and Gotoh ( $R_\lambda = 380$ ,  $a \in [-150, 150]$ ) [21]; the classical Reynolds number is  $\text{Re} = R_\lambda^2/15$ . This gives an important information on the dynamics and new look to the intermittency in high-Reynolds-number fluid turbulence.

Response characteristics of the polystyrene tracer particle of about  $46 \mu\text{m}$  size and the precision in the experiments [17,18] allow to resolve about 1/20 of the Kolmogorov time and 1/20 of the Kolmogorov length in an  $R_\lambda = 970$  flow so that the acceleration can be really resolved, and the particle follows rare violent events within 7% of the ideal value of acceleration even at the highest Reynolds number studied there. For lower Reynolds numbers the resolutions with respect to Kolmogorov scales are even much higher. The collected statistics of about  $1.7 \times 10^8$  data points appeared to be sufficient to establish finiteness of the fourth-order moment of the acceleration,  $\langle a^4 \rangle$ . The acceleration values are obtained from the measured velocity increments in time by certain extrapolation to zero-time increment, a procedure requiring handling data points in the dissipative scale [17,20].

The stretched exponential fit with three parameters provides a good agreement with the experimental data on the transverse acceleration  $a$  of the tracer particle in the  $R_\lambda = 690$  flow [17,20],

$$P(a) = C \exp\left[-\frac{a^2}{(1 + |b_1 a/b_2|^{b_3})b_2^2}\right], \quad (13)$$

where  $b_1 = 0.513 \pm 0.003$ ,  $b_2 = 0.563 \pm 0.02$ , and  $b_3 = 1.600 \pm 0.003$  are fit parameters and  $C = 0.733$  is a normalization constant. At large acceleration values the tails of the above  $P(a)$  decrease asymptotically as  $\exp[-|a|^{0.4}]$ , which implies a convergence of the fourth-order moment,  $\langle a^4 \rangle = \int_{-\infty}^{\infty} a^4 P(a) da$ . The flatness factor of the distribution (13) which characterizes the widening of its tails (when compared with a Gaussian) is

$$F \equiv \frac{\langle a^4 \rangle}{\langle a^2 \rangle^2} \approx 55.1, \quad (14)$$

which should be compared with the flatness of the experimental curve,  $F = 55 \pm 8$  [20]. We remind that for a Gaussian distribution  $F = 3$ .

With constant  $\beta$ , the Gaussian probability density function (6) corresponds to the non-intermittent Kolmogorov 1941 picture of fully developed turbulence, and agrees with the experimental statistics of components of velocity increments in time for large time scales, up to the integral time scale. However, it fails to describe observed Reynolds-number dependent stretched exponential tails of the experimental acceleration probability density function (13) that correspond to anomalously high probabilities for the tracer particle to have extremely high accelerations, bursts with dozens of root-mean-square (rms) acceleration, in the developed turbulent flow. Such a high probability of the extreme acceleration magnitudes is associated with the Lagrangian turbulence intermittency, which was found to be considerably stronger than the Eulerian one. Equivalently, one can say that it is related to an increase of the probability to have large velocity increments in time with a decrease of the time scale, down to the Kolmogorov time scale (a statistical viewpoint).

In the Eulerian framework, the turbulence intermittency is usually understood differently, as an increase of the probability to have large longitudinal velocity differences at short spatial scales, and studied through nonlinearity in scaling exponents of velocity structure functions (a structural viewpoint).

Intermittency of the stochastic energy dissipation rate is related to the dynamical intermittency of chaoticity in the system that makes a link between the Eulerian and Lagrangian intermittency to which we refer below.

The averaging (1) of the Gaussian distribution (6) over randomly distributed  $\beta$ , an evaluation of the stochastic expectation, was found to be a simple *ad hoc* procedure to obtain observable predictions, with one free parameter, that meet experimental statistical data on the acceleration of the tracer particle. One can think of this as the averaging over a large time span for one tracer particle, or as the averaging over an ensemble of tracer particles, moving in the three-dimensional flow characterized by random spatially distributed domains with different values of  $\beta$ .

Physically one would like to know the processes underlying the random character of the model parameter  $\beta$ . Due to the definition (4) the random character of  $\beta$  is attributed to a random character of the drift coefficient  $\gamma$  and/or the additive noise intensity  $\sigma^2$ .

The distribution of  $\beta$  is not fixed uniquely by the theory so that a judicious choice of  $f(\beta)$  makes a problem in the RIN model (1)–(6).

The primary aim of the present work is to provide a critical evaluation of the Langevin modeling approach by making a comparative analysis of different types of models on the basis of recent Lagrangian experimental data.

The crucial point is to make a link between the Langevin-type equation and the Navier-Stokes equation. This includes determination of statistical properties of stochastic terms and the functional form of deterministic terms, as well as their dependence on the parameters entering the Navier-Stokes equation justified for the inertial range of fully developed turbulence. Also, some extension of the stochastic equation may be required to account for dependence of the parameters

on Lagrangian velocity fluctuations, in the spirit of second-order stochastic models [15] and in correspondence to the Navier-Stokes equation as the pressure gradient term in the Eulerian framework can be expressed in terms of the velocity owing to the incompressibility condition. Strong and nonlocal character of Lagrangian particle coupling due to pressure effects makes the main obstacle to derive turbulence statistics from the Navier-Stokes equation. The layout of the paper is as follows.

In Sec. II we review some recent one-dimensional Langevin models of the developed turbulence.

In Sec. II A, we outline implications of the RIN models with the underlying  $\chi$ -square (Sec. II A 1) and log-normal (Sec. II A 2) distributions of  $\beta$  [5,6,11]. We review results of a recent approach [12] to specify  $f(\beta)$  which is based upon relating  $\beta$  to velocity fluctuations  $u$  and using normal distribution of velocity fluctuations with zero mean (Sec. II A 3). This enables to reproduce  $\chi$ -square and log-normal distributions of  $\beta$  as particular cases. In general, this approach assumes that parameters of the model, such as the intensity of additive noise, depend on velocity fluctuations, in an agreement with the Heisenberg-Yaglom picture of developed turbulence.

A nonlinear Langevin and the associated Fokker-Planck equations obtained by a direct requirement that the probability distribution satisfies some model-independent scaling relation have been recently proposed by Hnat, Chapman, and Rowlands [22] to describe the measured time series of the solar wind bulk plasma parameters. We find this result relevant to fluid turbulence since it is based on a stochastic dynamical framework and leads to the stationary distribution with exponentially truncated power-law tails, similar to that obtained in the above mentioned RIN models (Sec. II B).

The above one-dimensional Langevin toy models of Lagrangian turbulence all suffer from the lack of physical interpretation, e.g., of short term dynamics, or small-scale and large-scale contributions, in the context of three-dimensional Navier-Stokes equation.

The Navier-Stokes equation based approach to describe statistical properties of small-scale velocity increments, both in the Eulerian and Lagrangian frames, was developed in much detail by Laval, Dubrulle, and Nazarenko [23]; see also recent work [24]. This approach introduces nonlocal interactions between well separated large and small scales, elongated triads, and is referred to as the rapid distortion theory (RDT) approach. This approach is contrasted with the Gledzer-Ohkitani-Yamada shell model, in which interactions of a shell of wave numbers with only its nearest and next-nearest shells are taken into account. We outline results of this approach and focus on the proposed one-dimensional Langevin model of Lagrangian turbulence which we refer to as the Laval-Dubrulle-Nazarenko (LDN) model (Sec. II C). Particularly, we calculate exactly the probability density function of acceleration stemming from this model.

In Sec. III we make qualitative and quantitative comparative analysis of the one-dimensional LDN and simple RIN models.

In Sec. IV we study conditional probability density function  $P(a|u)$  taking the LDN model with  $\delta$ -correlated noises

and assuming that the additive noise intensity parameter  $\alpha$  depends on the amplitude of velocity fluctuations  $u$ .

## II. ONE-DIMENSIONAL LANGEVIN MODELS OF THE LAGRANGIAN TURBULENCE

In this section, we outline results of some recent one-dimensional Langevin models of the Lagrangian fluid particle acceleration in the developed turbulent flow.

### A. Simple RIN models

#### 1. The underlying $\chi$ -square distribution

With the underlying  $\Gamma$  ( $\chi$ -square) distribution of  $\beta$  of order  $n$  ( $n=1,2,3,\dots$ ),

$$f(\beta) = \frac{1}{\Gamma\left(\frac{n}{2}\right)} \left(\frac{n}{2\beta_0}\right)^{n/2} \beta^{(n/2)-1} \exp\left[-\frac{n\beta}{2\beta_0}\right], \quad (15)$$

the resulting marginal probability density function (1) with  $P(a|\beta)$  given by the Gaussian (6) is found in the form (cf. Ref. [6])

$$P(a) = \frac{C}{(a^2 + n/\beta_0)^{(n+1)/2}}, \quad (16)$$

where

$$C = \frac{(n/\beta_0)^{n/2} \Gamma\left(\frac{n+1}{2}\right)}{\sqrt{\pi} \Gamma\left(\frac{n}{2}\right)} \quad (17)$$

is normalization constant. With  $n=3$  ( $\beta_0=3$  for a unit variance) one obtains the normalized marginal distribution in the following simple form:

$$P(a) = \frac{2}{\pi(a^2 + 1)^2}, \quad (18)$$

a prediction of the  $\chi$ -square model, with the Tsallis entropic index taken to be  $q=(n+3)/(n+1)=3/2$  due to the theoretical argument that the number of independent random variables at Kolmogorov scale is  $n=3$  for the three-dimensional flow [6]. One can see that the resulting marginal distribution is characterized by power-law tails that *a priori* lead to divergent higher moments.

A Gaussian truncation of the power-law tails naturally arises under the assumption that the parameter  $\beta$  contains a nonfluctuating part, which can be separated out as follows:  $\beta/2 \rightarrow a_c^{-2} + \beta/2$  [11]. This leads to the modified marginal distribution

$$P(a) = \frac{C \exp[-a^2/a_c^2]}{(a^2 + n/\beta_0)^{(n+1)/2}}, \quad (19)$$

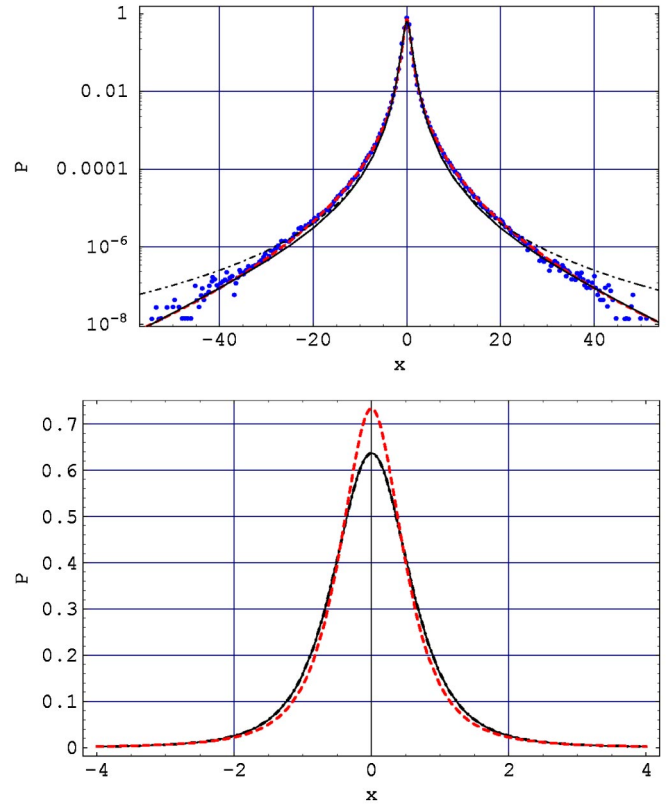


FIG. 1. Acceleration probability density function  $P(a)$ . Dots: experimental data at  $R_\lambda=690$  by Crawford, Mordant, and Bodenschatz [18]. Dashed line: stretched exponential fit (13),  $b_1=0.513$ ,  $b_2=0.563$ ,  $b_3=1.600$ ,  $C=0.733$ . Dot-dashed line: Beck  $\chi$ -square model (18),  $q=3/2$ . Solid line:  $\chi$ -square Gaussian model (19),  $a_c=39.0$ ,  $C=0.637$ .  $x=a/\langle a^2 \rangle^{1/2}$  denotes normalized acceleration.

where  $C$  is normalization constant and  $a_c > 0$  is a free parameter which can be used for a fitting. Taking the theoretical value  $n=3$  and  $\beta_0=3$  as in the above case, one obtains that

$$C = \frac{2a_c^2}{\pi(a_c^2 - 2) \exp[a_c^{-2}] [1 - \text{erf}(a_c^{-1})] + 2\sqrt{\pi} a_c}, \quad (20)$$

where  $\text{erf}(x)$  denotes the error function. The distribution (19) at the fitted value  $a_c=39.0$  is in a good agreement with the experimental probability density function  $P(a)$  [17,18].

Note that at  $a_c \rightarrow \infty$  (no constant part) the model (19) covers the model (16). Within the framework of Tsallis nonextensive statistics, the parameter  $q-1$  measures a variance of fluctuations. For  $q \rightarrow 1$  (no fluctuations), Eq. (19) reduces to a Gaussian distribution, which meets the experimental data for temporal velocity increments at the integral time scale.

A comparison of the  $\chi$ -square model (18) and  $\chi$ -square Gaussian model (19) with the experimental data is shown in Figs. 1 and 2. One can see that both the distributions follow the experimental  $P(a)$  to a good accuracy (at least up to 3 standard deviations), although the tails of the  $\chi$ -square model distribution departure to the experimental curve at big  $|a|$ . A major difference is seen from the contribution to the fourth-order moment  $a^4 P(a)$  shown in Fig. 2. The  $\chi$ -square model

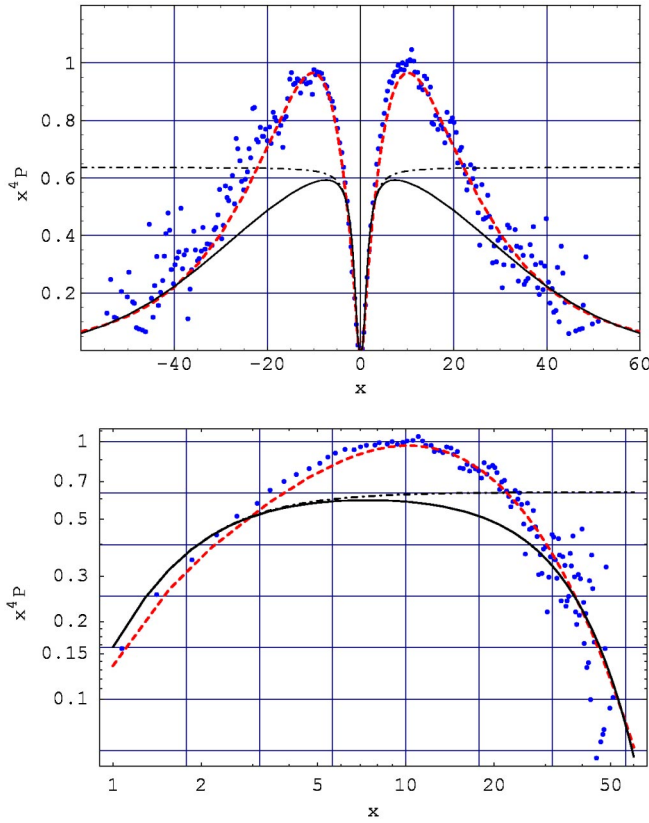


FIG. 2. Contribution to the fourth-order moment  $a^4 P(a)$ . Top panel, a linear plot, bottom panel: a log-log plot. Notation is the same as in Fig. 1.

yields a qualitatively unsatisfactory behavior indicating a divergency of the predicted fourth-order moment. In contrast, the  $\chi$ -square Gaussian model is in a good qualitative agreement with the data, reproducing them well at small and large acceleration values although quantitatively it deviates at intermediate acceleration values and gives the flatness value  $F \approx 46.1$  for  $a_c = 39.0$ , as compared to the flatness value (14).

## 2. The underlying log-normal distribution

With the underlying log-normal distribution of  $\beta$ ,

$$f(\beta) = \frac{1}{\sqrt{2\pi s\beta}} \exp\left[-\frac{\left(\ln\frac{\beta}{m}\right)^2}{2s^2}\right], \quad (21)$$

the resulting marginal probability density function (1) with  $P(a|\beta)$  given by the Gaussian (6) was recently proposed to be [5]

$$P(a) = \frac{1}{2\pi s} \int_0^\infty d\beta \beta^{-1/2} \exp\left[-\frac{\left(\ln\frac{\beta}{m}\right)^2}{2s^2}\right] e^{-1/2\beta a^2}, \quad (22)$$

where the only free parameter  $s$  can be used for a fitting, or derived from theoretical arguments,  $s^2 = 3$  ( $m = \exp[s^2/2]$  for a unit variance). This distribution is shown in Fig. 3 and was

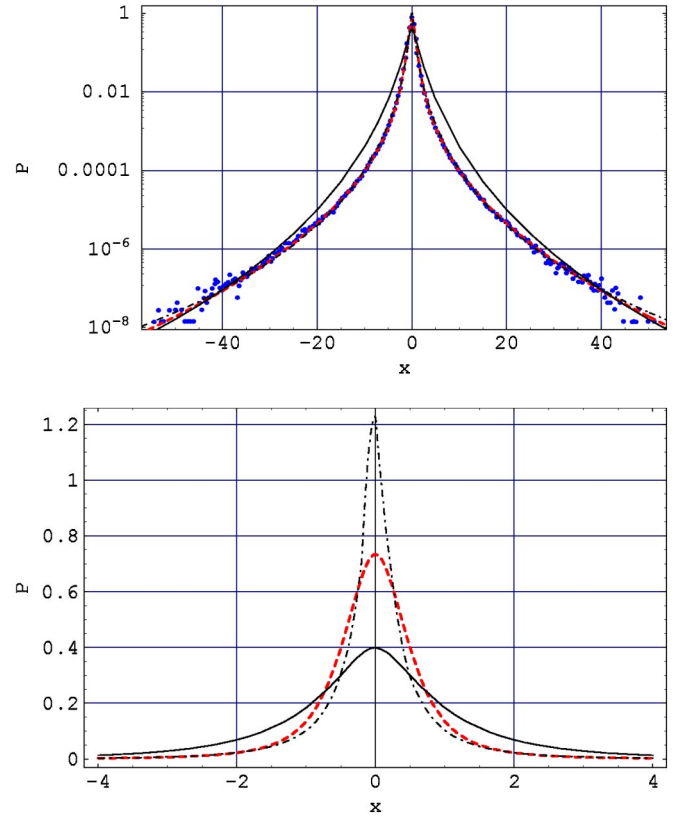


FIG. 3. Acceleration probability density function  $P(a)$ . Dots: experimental data at  $R_\lambda = 690$  by Crawford, Mordant, and Bodenschatz [18]. Dashed line: stretched exponential fit (13),  $b_1 = 0.513$ ,  $b_2 = 0.563$ ,  $b_3 = 1.600$ ,  $C = 0.733$ . Dot-dashed line: Beck log-normal model (22),  $s = 3.0$ . Solid line: Castaing log-normal model (23),  $s_0 = 0.625$ .  $x = a/\langle a^2 \rangle^{1/2}$  denotes normalized acceleration.

found to be in a good agreement with the Lagrangian experimental data by Porta *et al.* [17], the new data by Crawford *et al.* [18], Mordant *et al.* [19], and direct numerical simulations (DNS) of the Navier-Stokes equation by Kraichnan and Gotoh [21].

However, the central part of the distribution shown in the bottom panel of Fig. 3 reveals greater inaccuracy of the log-normal model [ $P(0) \approx 1.23$ ] as compared with that of both the  $\chi$ -square and  $\chi$ -square Gaussian models [ $P(0) \approx 0.65$ ] which are almost not distinguishable in the region  $|a|/\langle a^2 \rangle^{1/2} \leq 4$  (the bottom panel of Fig. 1); see also recent work by Gotoh and Kraichnan [13]. This is the main failing of the log-normal model (22) for  $s^2 = 3.0$  although the predicted distribution follows the measured low probability tails, which are related to the Lagrangian intermittency, to a good accuracy. The central region of the experimental curve (13) [ $P(0) \approx 0.73$ ] contains most weight of the experimental distribution and is the most accurate part of it, with the relative uncertainty of about 3% for  $|a|/\langle a^2 \rangle^{1/2} < 10$  and more than 40% for  $|a|/\langle a^2 \rangle^{1/2} > 40$  [20].

The distribution (22) is characterized by a bit bigger flatness value,  $F = 3 \exp[s^2] \approx 60.3$  for  $s^2 = 3$ , as compared to the flatness value (14), which is nevertheless acceptable from the experimental point of view. The peaks of the contribution to

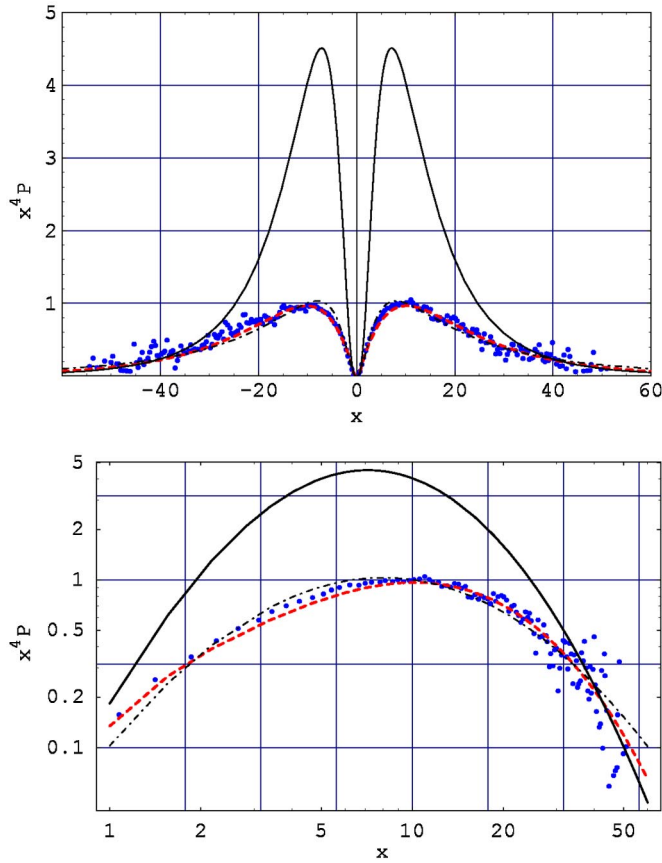


FIG. 4. Contribution to the fourth-order moment  $a^4 P(a)$ . Top panel, a linear plot; bottom panel, a log-log plot. Notation is the same as in Fig. 3.

fourth-order moment shown in Fig. 4 do not match that of the experimental curve for the  $R_\lambda = 690$  flow. We note that the best fit is achieved for  $s^2$  close to the theoretical value 3 but this does not significantly improve overlapping of the peaks with the data points.

One naturally expects that a better correspondence to the experiment may be achieved by an accounting for small-scale interactions via turbulent viscosity [certain nonlinearity in the first term on the rhs of Eq. (2)] as it implies a damping of the large events, i.e., less pronounced enhancement of the tails of  $P(a)$ .

It should be noted that the idea to describe turbulence intermittency via averaging of the Gaussian distribution over log normally distributed variance of some intermittent variable was proposed a long time ago by Castaing, Gagne, and Hopfinger [14],

$$P(x) = \frac{1}{2\pi s_0} \int_0^\infty d\theta \theta^{-2} \exp\left[-\frac{\left(\ln\frac{\theta}{m_0}\right)^2}{2s_0^2}\right] e^{-x^2/(2\theta^2)}, \quad (23)$$

where  $x$  is a variable under study. Below, we apply this model to the Lagrangian acceleration,  $x = a$ .

In technical terms, the difference from the Castaing log-normal model is that in Eq. (22) the *inverse* square of the

variance,  $\beta = \theta^{-2}$ , is taken to be log normally distributed. In essence, the models (22) and (23) are of the same type, with different parameters assumed to be fluctuating at a large time scale and hence different resulting marginal distributions.

One can check that the change of variable,  $\theta = \beta^{-1/2}$ , in Eq. (23) leads to the density function different from that given by Eq. (22),

$$P(x) \approx \int_0^\infty d\beta \beta^{-3/2} \exp\left[-\frac{\left(\ln\frac{\beta}{m_1}\right)^2}{2s_1^2}\right] e^{-(1/2)\beta x^2}, \quad (24)$$

where we have denoted  $m_1 = m_0^{-2}$  and  $s_1 = 2s_0$ . Therefore, the distributions (22) and (23) are indeed not equivalent to each other, both being of a stretched exponential form.

As to a comparison of the fits, we found that the fit of the Castaing log-normal model (23) for the acceleration, with the fitted value  $s_0 = 0.625$  ( $m_0 = \exp[s_0^2/2]$  for unit variance), is of a considerably lesser quality as one can see from Fig. 3 and, more clearly, from Fig. 4. Positions of the peaks of  $a^4 P(a)$  are approximately the same for both the models, namely,  $|a|/\langle a^2 \rangle^{1/2} \approx 8$  as compared to  $|a|/\langle a^2 \rangle^{1/2} \approx 10.2$  for the experimental curve.

We conclude this section with the following remark. The Langevin model of the type (2), Fokker-Planck approximation of the type (5), and the underlying log-normal distribution (21) within the Castaing approach were recently used by Hnat, Chapman, and Rowlands [22] to describe intermittency and scaling of the solar wind bulk plasma parameters.

### 3. The underlying Gaussian distribution of velocity fluctuations

The problem of selecting appropriate distribution of the parameter  $\beta$  among possible ones was recently addressed in Ref. [12]. A specific model based on the assumption that the velocity fluctuation  $u$  follows normal distribution with zero mean and variance  $s$  was developed. The result is that a class of underlying distributions of  $\beta$  can be encoded in the function  $\beta = \beta(u)$ , and the marginal distribution is found to be

$$P(a) = C(s) \int_0^\infty d\beta P(a|\beta) \exp\left[-\frac{[u(\beta)]^2}{2s^2}\right] \left|\frac{du}{d\beta}\right|, \quad (25)$$

where  $u(\beta)$  is the inverse function. Note that only an *absolute* value of  $u$  contributes to this probability distribution. Particularly, the exponential dependence

$$\beta(u) = \exp[\pm u], \quad (26)$$

features the log-normal distribution of  $\beta$  so that Eq. (25) leads to Eq. (22) used in Ref. [5], while the  $\chi^2$  distribution of order 1 is recovered with

$$\beta(u) = u^2. \quad (27)$$

In general, this model is relevant when  $\beta(u)$  is a monotonic Borel function of the stochastic variable  $u$  mapping  $[-\infty, \infty] \ni u$  to  $[0, \infty] \ni \beta$ , and allows one to rule out some

*ad hoc* distributions of  $\beta$  as well as to make appropriate generalizations of both  $\chi^2$  and log-normal distributions of the parameter  $\beta$ .

Below, we develop a possible dynamical foundation of the above model.

The stationary distribution (25) with  $\beta(u) = \exp[\pm u]$  can be associated to the Langevin equation of the form [12]

$$\partial_t a = \gamma F(a) + e^\omega L(t), \quad (28)$$

where we denote  $\omega = \mp u/2$ ,  $u$  follows Gaussian distribution with zero mean, and we take  $\gamma = \text{const}$  to simplify the consideration.

In general, we adopt a viewpoint that statistical properties of the acceleration  $a$  are associated with velocity fluctuation statistics due to the well-known Heisenberg-Yaglom theory. This theory predicts the following scaling of a component of the acceleration variance:

$$\langle a^2 \rangle = a_0 \bar{u}^{9/2} \nu^{-1/2} L^{-3/2}, \quad (29)$$

where  $\bar{u}$  is the rms velocity,  $L$  is the integral scale length, and  $a_0$  is the Kolmogorov constant. This long-standing universal  $\bar{u}^{9/2}$  scaling was confirmed by the recent Lagrangian experiments [17] to a very high accuracy, for about seven orders of magnitude in the acceleration variance, or two orders of the rms velocity, at  $R_\lambda > 500$ . At lower Reynolds numbers,  $R_\lambda < 500$ , it appeared that the Heisenberg-Yaglom scaling significantly deviates from the experimental data due to the emerging dependence of  $a_0$  on  $R_\lambda$  (the acceleration is increasingly coupled to large scales of the flow at low Reynolds numbers).

We note also that in the Sawford model the Langevin equation (10) for  $a$  includes velocity fluctuations  $u$  and the variance of the velocity distribution.

Below, we outline a relationship of the model (28) to some recent approaches in studying the intermittency.

(i) The form of the last term in Eq. (28), in which  $\omega$  can be viewed as a Gaussian process,  $\omega = \omega(t)$ , independent of the white noise  $L(t)$ , strikingly resembles that involved in the recently developed log-infinitely divisible multifractal random walks (MRW) model by Muzy and Bacry [25], a continuous extension of discrete cascades.

(ii) The driving force amplitude of the form  $e^{\omega(t)}$ , with an ultraslow decaying correlation function,  $\langle \omega(t)\omega(t+\tau) \rangle_t = -\lambda_0^2 \ln[\pi T_L]$ ,  $\tau < T_L$ , in the Langevin-type equation has been recently considered by Mordant *et al.* [19];  $T_L$  stands for the Lagrangian integral time. The results of this model have been found in a very good agreement with the experimentally observed very slow decay of the equal-position time autocorrelation of the fluid particle velocity increment magnitude in time  $|\Delta_\tau u_i|$  for each component (very much similar to MRW model) attributed to the intermittency of Lagrangian trajectories in the developed turbulent flow. Also, very slow decay was observed for the cross correlation of the magnitudes of the acceleration components. Both the dynamical correlations were found to vanish only for  $\tau > 3T_L$ , while the dynamical correlations of the full signed entities,  $\Delta_\tau u_i$ , decay

rapidly, the autocorrelation functions cross zero at about  $\tau \approx 0.06T_L$ , and the cross correlation functions are approximately zero.

We note that the fitted value of the above intermittency parameter  $\lambda_0$  ( $\lambda_0^2 = 0.115 \pm 0.01$ ) is very close to  $1/s^2 = 1/3$ , with the value  $s^2 = 3$  in Eq. (22) interpreted as the number of independent random variables in three-dimensional space at the Kolmogorov scale. If this is not due to a coincidence, the intermittency parameter  $\lambda_0$  approaches simply the inverse of the effective space dimension number  $d$ ,

$$\lambda_0 = 1/d, \quad (30)$$

$d = 3$ , for high-Reynolds-number turbulent flows.

The above connection to the MRW model and very slow decay of the correlations of the absolute values of acceleration components indicate relevance of the specific representation (28), with very slow varying  $|u|$ , in the description of intermittency. In fact, due to the experiments [26] the Lagrangian velocity auto correlation function  $\langle u(t)u(t+\tau) \rangle_t / \langle u^2 \rangle$  decays almost exponentially but very slowly, to vanish only for  $\tau > 3T_L$ , where the integral time scale  $T_L = 2.2 \times 10^{-2}$  s, which is two orders of magnitude bigger than the Kolmogorov time scale  $\tau_\eta = 2.0 \times 10^{-4}$  s,  $R_\lambda = 740$ , and the mean velocity is about 10% of the rms velocity.

(iii) Due to the well-known Kolmogorov power-law scaling relationship between  $\bar{\epsilon}$  and  $\bar{u}$ , the representation (28) can be thought of as the result of using the relation  $\ln \beta \approx \ln \epsilon$ , with  $\ln \epsilon$  being normally distributed due to the refined Kolmogorov 1962 theory. Here,  $\epsilon$  denotes the stochastic energy dissipation rate per unit mass treated in the Lagrangian framework. From this point of view, one can identify

$$\omega = g \ln \epsilon, \quad (31)$$

where  $g$  is a constant. This means that the stochastic dynamics of the logarithm of the energy dissipation is independent, and it influences the acceleration dynamics specifically through the intensity of driving stochastic force in Eq. (28). Stationary normal distribution of  $\omega$  can be in turn derived from the Fokker-Planck equation associated with the Langevin equation of a linear form,

$$\partial_t \omega = g_0 + g_1 \omega + g_2 L(t), \quad (32)$$

where  $g_i$  are constants. This equation is in an agreement with the recent results of Eulerian (hotwire anemometer) study of the interaction between velocity increments and normalized energy dissipation rate by Renner, Peinke, and Friedrich [27]. Particularly, they found that an exponential dependence of the diffusion coefficient on the logarithmic energy dissipation in the Fokker-Planck equation for the velocity increments in space is in a very good agreement with the experimental data. We note that Eq. (32) does not imply a logarithmic decay of the Lagrangian correlation function  $\langle \omega(t)\omega(t+\tau) \rangle$  proposed in Ref. [19]. This may be attributed to the well-known difference between the Eulerian (fixed probe) and Lagrangian (trajectory) frameworks.



(iv) For the choice  $\beta(u) = \exp[u]$  corresponding to the log-normal distribution of  $\beta$ , using Eq. (28) one can derive the stationary probability density function of the form [12]

$$P(a) = \int_{-\infty}^{\infty} du C(u) \exp\{\ln[g(u)] - e^u a^2/2\}, \quad (33)$$

where  $g(u)$  is a probability density function of  $u$ . Hence the joint probability density function can be written as

$$P(a, u) = C(u) \exp\{\ln[g(u)] - e^u a^2/2\}. \quad (34)$$

Such a form of the distribution, containing specifically the double exponent, resembles the ‘‘universal’’ distribution of fluctuations (Gumbel function)

$$P(x) = c_0 \exp[c_1(y - e^y)], \quad y \equiv c_2(x - c_3), \quad (35)$$

where  $c_i$  are constant, recently considered by Chapman, Rowlands, and Watkins [28] (see also references therein) following the work by Portelli, Holdsworth, and Pinton [29]. They used an apparently different approach (not related to a Langevin-type equation for the acceleration studied in our paper) based on the multifractal-type energy cascade and  $\chi^2$  or log normal (Kolmogorov 1962 theory) underlying distribution for the energy dissipation rate at fixed level. They pointed out a good agreement of such  $P(x)$  with experimental data, where  $x$  denotes a fluctuating entity observed in a variety of model correlated systems, such as turbulence, forest fires, and sandpiles. The result of this approach meets ours and we consider it as an alternative way to derive the characteristic probability measure of fluctuations; with  $g(u)$  taken to be a  $\chi^2$  (respectively, Gaussian) density function, one obtains, up to a preexponential factor and constants,  $P(u) \sim \exp(-u - \exp[u])$   $\{P(u) \sim \exp(-u^2 - \exp[u])\}$ . Thus we conclude that the universal distribution (35) can be derived also within the general framework proposed in Ref. [12] that reflects a universal character of the underlying  $\chi^2$  distribution [4].

We note that although successful in describing the observed statistics of Lagrangian acceleration, with a few simple hypotheses and one fitting parameter, the one-dimensional Langevin RIN models (1)–(5) and (25)–(28) suffer from the lack of physical interpretation in the context of the three-dimensional Navier-Stokes equation.

In summary, we have presented a class of models (25)–(28) using the basic assumption that the parameter  $\beta$  depends on normally distributed velocity fluctuations. This class has been found to incorporate the previous RIN models in a unified way, with the dependence  $\beta(u)$  required to be a (monotonic) Borel function of the stochastic variable  $u$ .

### B. Hnat-Chapman-Rowlands model

Another interesting model developed recently by Hnat, Chapman, and Rowlands [22] to describe the observed time series of the solar wind bulk plasma parameters is based on the construction of Fokker-Planck equation for which the probability density function obeys the following one-parametric model-independent rescaling:

$$P(x, t) = t^{-\alpha_0} P_s(xt^{-\alpha_0}), \quad (36)$$

where  $x$  denotes fluctuating plasma parameter and  $\alpha_0$  is the scaling index. The value  $\alpha_0 = 1/2$  corresponds to a self-similar Brownian walk with Gaussian probability density functions at all time scales. The fitted value  $\alpha_0 = 0.41$  corresponds to a single non-Gaussian distribution  $P_s(x_s)$ , to which the observed distributions of some four plasma parameters collapse under the scaling,  $x_s = xt^{-\alpha_0}$ .

The Langevin equation of this model assumes only additive noise, and in such an ansatz it was found to be

$$\partial_t x = D_1(x) + D_2(x) \eta(t), \quad (37)$$

where  $D_1$  and  $D_2$  are of the form

$$D_1(x) = \sqrt{\frac{b_0}{D_0}} x^{1-\alpha_0^{-1}/2}, \quad (38)$$

$$D_2(x) = [b_0(1 - \frac{1}{2}\alpha_0^{-1}) - a_0] x^{1-\alpha_0^{-1}}, \quad (39)$$

$a_0, b_0$  are constants and  $2D_0$  is intensity of the  $\delta$ -correlated Gaussian-white additive noise  $\eta(t)$ ,  $\langle \eta(t) \rangle = 0$ . By construction, this specified form of the dynamical equation ensures that the corresponding Fokker-Planck equation

$$\partial_t P(x, t) = \partial_x [a_0 x^{1-\alpha_0^{-1}} P + b_0 x^{2-\alpha_0^{-1}} \partial_x P] \quad (40)$$

has the general solution  $P(x, t)$ , which exhibits the scaling (36). The fitted values are  $a_0/b_0 = 2$ ,  $b_0 = 10$ , and  $\alpha_0^{-1} = 2.44$ . The rescaled distribution  $P_s(x_s)$  corresponding to Eq. (40) is characterized by power-law tails truncated by stretched exponential with a good fit to the tails of the experimental distribution, but it *diverges* at the origin,  $x_s \rightarrow 0$ .

To sum up, we point out that this diffusion model uses the generalized self-similarity principle resembling that used in the Eulerian description of the energy cascade in the developed three-dimensional fluid turbulence and appears to be valid only asymptotically for large values of the variable, with the fitted parameter value being about  $\alpha_0 = 0.41$ .

### C. Laval-Dubrulle-Nazarenko model

The Navier-Stokes equation based approach to describe statistical properties of small-scale velocity increments, both in the Eulerian and Lagrangian framework, was developed in much detail by Laval, Dubrulle, and Nazarenko [23]; see also recent work [24]. This approach is based on featuring nonlocal interactions between well separated large and small scales, elongated triads, and is referred to as the RDT approach. Decomposition of velocities into large- and small-scale parts was made by introducing a certain spatial filter of a cutoff type. Within the framework of this approach, a three-dimensional Langevin model of the developed turbulence was proposed.

In its one-dimensional version, the toy model of the Lagrangian turbulence naturally implies a nonlinear Langevin-type equation for a component of the small-scale velocity increments in time (in the zero time-scale limit it corresponds to the acceleration  $a$  of fluid particle) [23],

$$\partial_t a = (\xi - \nu_t k^2) a + \sigma_\perp. \quad (41)$$

This equation is a Lagrangian description in the scale space, in the reference frame comoving with a wave number packet. Here,

$$\nu_t = \sqrt{\nu_0^2 + B^2 a^2 / k^2} \quad (42)$$

stands for the turbulent viscosity introduced to describe small-scale interactions,  $\nu_0$  is kinematic viscosity,  $B$  is constant,  $k$  is wave number [ $\partial_t k = -k\xi$ ,  $k(0) = k_0$ , to model the RDT stretching effect in one-dimensional case],  $\xi$  and  $\sigma_\perp$  are multiplicative and additive noises associated with the velocity derivative tensor and forcing of small scales by large scales (the energy transfer from large to small scales), respectively.

We refer to the model (41) as the one-dimensional LDN model of the developed Lagrangian turbulence. This toy model can also be viewed as a passive scalar in a compressible one-dimensional flow.

The noises, one-dimensional versions of which appear in Eq. (41), are projections related to the large-scale velocities  $U_i$  and small-scale velocities  $u_i$  of the flow as follows [23]:

$$\hat{\xi} = \vec{\nabla} \cdot \left( \frac{2\vec{k}}{k^2} (\vec{k}\vec{U}) - \vec{U} \right), \quad (43)$$

$$\hat{\sigma}_\perp = \hat{\sigma} - \frac{\vec{k}}{k^2} (\vec{k}\hat{\sigma}), \quad (44)$$

$$\sigma_i = \partial_j (\overline{U_i U_j} - U_i U_j + \overline{u_j U_i} - \overline{U_j u_i}), \quad (45)$$

where the hat denotes Gabor transformation [30] and the bar stands for the spatial cutoff retaining the large-scale part. One can see that the noises are related to the velocity fluctuations and the additive noise contains interaction terms between the large- and small-scale dynamics.

This gives support to the idea that the intermittency is caused also by some nonlocal interactions within the inertial range and not merely by small scales. We remark that one would also like to know the role of the dissipative scale in this integrated picture.

Noisy character of the entities (43) and (44) may not be seen as a consequence of the Navier-Stokes equation, which does not contain external random forces at the characteristic time scale. In the RDT approach,  $\xi$  and  $\sigma_\perp$  are treated as independent stochastic processes entering the small-scale dynamics (41) owing to the fact that the large-scale dynamics is weakly affected by small scales (which corresponds to a direct energy cascade in the three-dimensional flow) and thus can be viewed as a given noise.

The relations (43) and (44) can be used to trace back the origin of the multiplicative and additive noises entering various surrogate Langevin models of the developed turbulence, and to provide important information on the dynamics underlying the intermittency.

Statistical properties of all the components of the noises  $\xi$  and  $\sigma_\perp$  were studied numerically for decaying turbulence and reveal rich and complex behavior, in the laboratory frame.

As a first step in the one-dimensional case, these noises were modeled in the Lagrangian frame by the coupled  $\delta$ -correlated Gaussian-white noises [23],

$$\langle \xi(t) \rangle = 0, \quad \langle \xi(t) \xi(t') \rangle = 2D \delta(t-t'),$$

$$\langle \sigma_\perp(t) \rangle = 0, \quad \langle \sigma_\perp(t) \sigma_\perp(t') \rangle = 2\alpha \delta(t-t'), \quad (46)$$

$$\langle \xi(t) \sigma_\perp(t') \rangle = 2\lambda \delta(t-t'),$$

where  $D$ ,  $\alpha$ , and  $\lambda$  are parameters depending on scale via  $k_0$ . The stationary solution of the Fokker-Planck equation associated with Eq. (41) with the noises (46),

$$\begin{aligned} \partial_t P(a, t) = & \partial_a (\nu_t k^2 P) + D \partial_a (a \partial_a P) - \lambda \partial_a (a \partial_a P) \\ & - \lambda \partial_a^2 (a P) + \alpha \partial_a^2 P, \end{aligned} \quad (47)$$

is given by [23]

$$P(a) = C \exp \left[ \int_0^a dy \frac{-\nu_t k^2 y - Dy + \lambda}{Dy^2 - 2\lambda y + \alpha} \right], \quad (48)$$

where  $C$  is a normalization constant and six parameters can be used to fit the experimental data. This model specifies the one-dimensional LDN model (41), and we refer to this model as the LDN model with  $\delta$ -correlated noises (dLDN model).

The Langevin equation containing both the  $\delta$ -correlated Gaussian-white multiplicative and additive noises was studied in detail by Nakao [31] (see also references therein) by using the associated Fokker-Planck equation. The dLDN model (41) extends Nakao's set up by incorporating two new features: (i) the nonlinearity controlled by  $B$  in Eq. (42) and (ii) the coupling of the noises controlled by  $\lambda$  in Eq. (46).

It is interesting to note that the RDT approach qualitatively resembles the model studied by Kuramoto and Nakao [32], a system of spatially distributed chaotic elements driven by a field produced by nonlocal coupling, which is spatially long-wave and temporally irregular. Such systems, in which the multiplicative noise is the local Lyapunov exponent fluctuating randomly due to the chaotic motion of the elements, show power-law correlations, intermittency, and structure functions similar to that of the developed fluid turbulence.

In the following section, we make a comparison of the RIN model (1)–(5) with the Laval-Dubrule-Nazarenko model (41), as well as its particular case, the dLDN model (48).

### III. COMPARISON OF THE SIMPLE RIN AND LDN MODELS

#### A. A qualitative comparison

A direct comparison of the Langevin equations (2) and (41) of the two models suggests the following evident identifications:

$$\gamma F(a) = (\xi - \nu_t k^2) a, \quad \sigma L = \sigma_\perp. \quad (49)$$

Hence the additive noises can be made identical to each other by putting  $\sigma^2 = \alpha$ . Further, in the case of a linear drift force,  $F(a) = -a$ , and constant viscosity,  $\nu_t = \nu_0$ , we can identify the remaining parameters,  $\gamma = \nu_0 k^2 - \xi$ , so that we get

$$\beta \equiv \gamma / \sigma^2 = (\nu_0 k^2 - \xi) / \alpha. \quad (50)$$

This relation implies that the parameter  $\beta$  can be viewed as a stochastic variable with a nonzero mean due to the stochastic nature of  $\xi$  assumed in the LDN model. This is in agreement with the simple RIN model, the defining feature of which is just that the fluctuating part of  $\beta$  follows some statistical distribution.

In the dLDN model (41)–(48), both the additive and multiplicative noises are taken  $\delta$  correlated due to Eq. (46). This is in a sharp contrast to the assumption that  $\beta$  can be taken constant to derive the stationary solution (6) which is the foundation of the simple RIN model. More precisely, the solution in the form (6) can be obtained as the lowest-order approximation if  $\beta$  is slow varying in time as compared to a typical time scale associated with the additive noise  $L(t)$  (the adiabatic approximation). This suggests that the multiplicative noise  $\xi$  should be taken as a sufficiently slow varying stochastic variable, to meet the ansatz used in the RIN model.

The detailed numerical analysis of the noises [23] for the turbulent flow at relatively low Reynolds numbers,  $57 < R_\lambda < 80$ , shows that the autocorrelation of the multiplicative noise  $\xi$  decays much slower (by about one order of magnitude) than that of the additive noise  $\sigma_\perp$ . Hence a typical time scale at which  $\xi$  varies,  $\tau_\xi$ , is considerably bigger than that,  $\tau_\sigma$ , of  $\sigma_\perp$ . Also, the cross correlation between the two noises was found to be rather weak,  $\lambda \ll D$  and  $\lambda \ll \alpha$ , by about two orders of magnitude in the longitudinal case and  $\lambda = 0$  in the transverse case. Altogether this allows one to introduce the time-scale hierarchy  $\tau_\xi \gg \tau_\sigma$  and to decouple the noises, i.e., to put  $\lambda = 0$ , which justifies the adiabatic approximation and the one-dimensional RIN model.

The presence of the long-time correlated amplitude  $e^{\omega(t)}$  and the short-time correlated directional part  $L(t)$  of the stochastic driving force in the Langevin-type equation considered by Mordant *et al.* [19] also supports the above adiabatic approximation (two well separated time scales in the single additive stochastic force, in the Lagrangian framework). As usual, the  $\delta$ -correlated noise originates from taking the limit of zero correlation time in a system with the smallest finite noise correlation time.

On the contrary, in the dLDN model one assumes the approximation of comparable time scales,  $\tau_\xi \simeq \tau_\sigma$ , and retains the coupling parameter  $\lambda$  relating small-scale stretching

and vorticity and responsible for the skewness, which is however quite small in homogeneous isotropic turbulent flows.

The use of the constant turbulent viscosity  $\nu_t = \nu_0$  makes a good approximation in describing intermittency corrections since both the constant and turbulent viscosities were found to produce corrections which are of the same level as the DNS result [23]. In the physical context, this means that the small-scale interactions are not of much importance in the dynamics underlying the intermittency. This justifies the use of the approximation of linear forcing  $F(a) = -a$  in the simple RIN model. We note that this is also in an agreement with both the experimental results for the Lagrangian velocity autocorrelation function by Mordant, Metz, Michel, and Pinton [26] and the recent experimental Eulerian results for the spatial velocity increments by Renner, Peinke, and Friedrich [27].

Alternatively, one can consider a *more general* RIN model characterized by the presence of  $\delta$ -correlated Gaussian-white additive and *multiplicative* noises and fluctuating intensities of both the noises. This will lead to a model similar to the dLDN model (41) in which the noise intensities  $D$  and  $\alpha$  and the coupling parameter  $\lambda$  are assumed to fluctuate at a large time scale.

In summary, we found that the one-dimensional RIN model (1)–(5) can be viewed as a particular case of the one-dimensional LDN model (41) of turbulence which is based on the RDT approach by Laval, Dubrulle, and Nazarenko [23]. It should be stressed that while both the toy models assume introduction of some external statistics—the correlator of  $L(t)$  and the distribution  $f(\beta)$  in Eq. (1) and the correlators of  $\xi$  and  $\sigma_\perp$  in Eq. (41)—the LDN model is characterized by a solid foundation and reveals a rich structure as compared to the RIN model.

In the first approximation, i.e.,  $\lambda = 0$ ,  $\nu_t = \nu_0$ , and  $\tau_\xi \gg \tau_\sigma$ , the class of RIN models is in a quite good qualitative correspondence with the LDN model (41) and differs from the specific dLDN model (41)–(48) by the only fact that in the latter one assumes  $\tau_\xi \simeq \tau_\sigma$  and introduces a  $\delta$ -correlated multiplicative noise. Hence the different resulting probability density functions for the acceleration of fluid particle in the developed turbulent flow, Eqs. (19)–(22) and (48), respectively.

#### B. A quantitative comparison

With the above result of the qualitative comparison, we are led to make a more detailed, quantitative comparison of the dLDN model (41)–(48) and the simple RIN model (1)–(5) with the underlying  $\chi^2$  or log-normal distribution of  $\beta$ , in order to determine which approximation,  $\tau_\xi \simeq \tau_\sigma$  or  $\tau_\xi \gg \tau_\sigma$ , is better when used to describe the Lagrangian statistical properties of the developed turbulent flow. We take the recent high precision Lagrangian experimental data [17,18] on statistics of fluid particle acceleration in the developed turbulent flow as a testbed. Actually we follow the remark made in Ref. [23] that the  $\delta$  approximation of  $\xi$  is debatable and the performance of such a model should be further examined in the future.

In Ref. [23], explicit analytic evaluation of the distribution (48) is given for the particular case  $\nu_t = \nu_0$ , while the general case is treated in terms of  $d \ln P(a)/da$  when fitting to the numerical RDT data ( $-4 \leq a \leq 4$ ). In order to make fits to the experimental probability density function  $P(a)$  and to the contribution to the fourth-order moment,  $a^4 P(a)$ , covering wide range of the normalized acceleration,  $-60 \leq a \leq 60$ , one needs an analytic or numerical evaluation of the rhs of Eq. (48). To this end, we have calculated *exactly* the integral appearing in the dLDN probability density function (48) (see the Appendix).

The  $\chi^2$  and log-normal distribution-based probability density functions (19) and (22) are both realizations of the RIN model and contain one fitting parameter,  $a_c$  and  $s$ , respectively. The result of comparison of fitting qualities of these functions [11], with  $a_c = 39.0$  and  $s = 3.0$ , is that the probability density function (22) provides a better fit to the experimental data [18] on low-probability tails and the contribution to the kurtosis summarizing the peakedness of distribution. However, since the integral in Eq. (22) cannot be evaluated analytically we will use the distribution (19), which provides a better fit to the central region when dealing with analytic expressions.

The dLDN probability density function (48) contains six parameters which can be used for a fitting, the multiplicative noise intensity  $D$ , the additive noise intensity  $\alpha$ , the coupling  $\lambda$  between the multiplicative and additive noises, the turbulent viscosity parameter  $B$ , the parameter  $\nu_0$ , and the wave number parameter  $k$ .

*The parameter  $k$ .* For a fitting, we can put  $k=1$  without loss of generality since it can be absorbed by the redefinition of the parameters  $\nu_0$  and  $B$ ,

$$\nu_0 k^2 \rightarrow \nu_0, \quad Bk \rightarrow B. \quad (51)$$

*The parameter  $\alpha$ .* The structure of the rhs of Eq. (48) is such that only four parameters out of five can be used for a fitting. For example, one can put  $\alpha=1$  without loss of generality by using the following redefinitions,

$$\nu_0/\alpha \rightarrow \nu_0, \quad B/\alpha \rightarrow B, \quad D/\alpha \rightarrow D, \quad \lambda/\alpha \rightarrow \lambda. \quad (52)$$

Alternatively, one can put  $D=1$  provided the redefinitions

$$\nu_0/D \rightarrow \nu_0, \quad B/D \rightarrow B, \quad \alpha/D \rightarrow \alpha, \quad \lambda/D \rightarrow \lambda. \quad (53)$$

*The parameter  $\lambda$ .* Due to Eq. (A5) we have  $c = -i\sqrt{D\alpha - \lambda^2}$ , which is purely imaginary for  $D\alpha > \lambda^2$  and real for  $D\alpha < \lambda^2$ . For  $c=0$ , i.e.,  $D\alpha = \lambda^2$ , the integral (A3) is finite since divergent  $F(c)$  and  $F(-c)$  defined by Eq. (A4) cancel each other. Since the parameter  $\lambda$  measuring the coupling between the noises is assumed to be much smaller than both the noise intensities  $D$  and  $\alpha$  [23], we put  $D\alpha > \lambda^2$  in our subsequent analysis. Moreover, the parameter  $\lambda$  responsible for the skewness can be set to zero since we will be interested, as a first step, in statistically isotropic and homogeneous turbulent flows, for which the experimental distribution  $P(a)$  exhibits very small skewness [17].

Thus, we can use three redefined free parameters  $\nu_0$ ,  $B$ , and  $D$  for a fitting, with  $k=1$ ,  $\alpha=1$ , and  $\lambda=0$ . However, we

shall keep  $k$  and  $\alpha$  in an explicit way in the formulas below, to provide a general representation.

We start by considering two important particular cases of the dLDN probability density function (48): a constant viscosity  $\nu_t = \nu_0$  and a dominating turbulent viscosity  $\nu_t = B|a|/k$ .

### 1. Constant viscosity

At  $\lambda=0$  (symmetric case) and  $B=0$ , i.e., constant viscosity  $\nu_t = \nu_0$ , using Eq. (A1) in Eq. (48) we get (cf. Ref. [23])

$$P(a) = C(Da^2 + \alpha)^{-(1 + \nu_0 k^2/D)/2}, \quad (54)$$

where  $C$  is normalization constant. This distribution is of a power-law-type and we can compare it with the result (19), which contains a Gaussian truncation of similar power-law tails.

We note that with the identifications

$$D/\alpha = 2(q-1), \quad (1 + \nu_0 k^2/D)/2 = 1/(q-1), \quad (55)$$

the distribution (54) coincides with that obtained in the context of generalized statistics with the underlying  $\chi^2$  distribution [6]. Particularly, for  $q=3/2$  ( $n=3$ ,  $\beta_0=3$ ) used there, it follows that  $D/\alpha=1$  and  $\nu_0 k^2=3$ .

It is highly remarkable to note that the two different approaches yield stationary distribution of exactly the same power law form for certain identification of the parameter's; namely, the Gaussian-white  $\delta$ -correlated multiplicative and additive noises with constant intensities and a linear drift term imply  $P(a)$  of the same form as that obtained in the RIN model with  $\chi^2$  distributed  $\beta$ , the ratio of the drift coefficient to the intensity of the Gaussian-white  $\delta$ -correlated additive noise. It follows that the effect of  $\chi^2$  distributed  $\beta$  mimics the presence of the multiplicative noise, and vice versa, in this particular case.

The power-law distribution (54) can be used to get a good fit of the Lagrangian experimental  $P(a)$  data for small accelerations, e.g., with the normalized values ranging from  $-10$  to  $10$ , but in contrast to the Gaussian truncated one (19) it exhibits strong deviations for large  $a$ , and for  $(1 + \nu_0 k^2/D)/2 \leq 2$  leads to a divergent fourth-order moment, which is known to be finite [11,17,10].

Introducing the noise intensity ratio parameter

$$b = \sqrt{D/\alpha} \quad (56)$$

and denoting

$$\kappa = -(1 + \nu_0 k^2/D)/2, \quad (57)$$

we can rewrite the normalized distribution (54) as follows (cf. Ref. [31]):

$$P(a) = \frac{(1 + b^2 a^2)^\kappa}{2 {}_2F_1\left(-\kappa; \frac{1}{2}; \frac{3}{2}; -b^2\right)}, \quad (58)$$

where  ${}_2F_1$  is the hypergeometric function. In accord to the analysis made by Nakao [31], for *small* additive noise inten-

sity, i.e., at  $b \gg 1$ , this distribution exhibits a pronounced plateau near the origin, and the  $n$ th order moments, *truncated* by reflective walls at some fixed  $|a|$ , behave as a power of  $b$ ,

$$\langle a^n \rangle \sim b^{-\nu_0 k^2/D} \quad \text{for } n > \nu_0 k^2/D, \quad (59)$$

$$\langle a^n \rangle \sim b^{-n} \quad \text{for } n < \nu_0 k^2/D, \quad (60)$$

where  $n > 0$ . Thus, the truncated moments behave as

$$\langle a^n \rangle \sim G_0 + G_1 b^{-H(n)}, \quad (61)$$

where  $G_{0,1}$  are some constants and the function  $H(n)$  is zero at  $\nu_0 k^2 = 0$  and monotonically saturates to  $n$  at big  $\nu_0 k^2$ . It should be stressed that such a behavior of the moments for small additive noise intensity is not specific to the distribution (58) since it gives divergent moments but arises after some truncation of it, for example, by means of reflective walls or nonlinearity. Particularly, a truncation of the power-law tails of the distribution naturally arises when accounting for the turbulent viscosity to which we turn below.

### 2. Dominating turbulent viscosity

At  $\lambda = 0$  (symmetric case), for the case of dominating turbulent viscosity,  $\nu_t = B|a|/k$ , using Eq. (A2) we get for positive and negative  $a$ , respectively,

$$P(a) = \frac{C e^{\mp Bka/D \pm Bk\alpha^{1/2} D^{-3/2} \arctan[(D/\alpha)^{1/2} a]}}{(Da^2 + \alpha)^{1/2}}, \quad (62)$$

where  $C$  is normalization constant. One can see that, as expected, the power-law dependence is of a similar form as in Eq. (54) but it is exponentially truncated at big  $|a|$  owing to the turbulent viscosity term. This distribution is similar to the Gaussian truncated one (19) but the truncation is of an exponential type and there is some symmetric enhancement of the tails supplied by the arctan term.

Now we turn to the general case, which provides a link between the two particular cases,  $\nu_t = \nu_0$  and  $\nu_t = B|a|/k$ , considered above.

### 3. The general symmetric case

At  $\lambda = 0$  (symmetric case), from Eqs. (A5)–(A7) we have

$$c = -id_2, \quad c_1 = id_1^2 d_2, \quad c_2 = kd_1, \quad (63)$$

where we have denoted

$$d_1 = \sqrt{D(Dk^2\nu_0^2 - B^2\alpha)}, \quad d_2 = \sqrt{D\alpha}. \quad (64)$$

Note that  $c$  is purely imaginary and the rhs of Eq. (A3) is much simplified yielding a symmetric distribution with respect to  $a \rightarrow -a$ . The entity  $c_2$  defined by Eq. (A7) may be either real (for  $Dk^2\nu_0^2 > B^2\alpha$ ) or purely imaginary (for  $Dk^2\nu_0^2 < B^2\alpha$ ). In particular, for the case of constant viscosity,  $\nu_0^2 \gg B^2$ , it is real while for the case of dominating turbulent part of the viscosity,  $B^2 \gg \nu_0^2$ , it is purely imaginary, provided that the intensities of noises,  $D$  and  $\alpha$ , are of the

same order of magnitude. These two particular cases lead to different final expressions for the distribution (54) and (62), respectively, obtained above.

In the general case, using Eqs. (63) and (64) in Eq. (A3) after some algebra we obtain the following expression for the dLDN probability density function (48), at  $\lambda = 0$ :

$$P(a) = \frac{C e^{-\nu_0 k^2/D}}{(Da^2 + \alpha)^{1/2}} \times \left[ \frac{4D^5(B^4D\alpha a^2 + k^2(Dk\nu_0^2 + d_1\nu_t)^2)}{d_1^6 k^2 (Da^2 + \alpha)} \right]^{kd_1/(2D^2)}, \quad (65)$$

where  $C$  is normalization constant,  $d_1$  is given in Eq. (64), and  $\nu_t$  is given by Eq. (42).

It can be easily checked that Eq. (65) reduces to Eq. (54) at  $B = 0$ , while to verify that it reduces to Eq. (62) at  $\nu_t = B|a|/k$  requires the use of the fact that  $d_1$  becomes purely imaginary, returning back to the logarithmic representation due to Eq. (A4), and the identity (A8).

The distribution (65) is characterized by the power-law tails, which are (i) exponentially truncated and (ii) enhanced by the power-law part of the numerator, with both the effects being solely related to the nonzero turbulent viscosity coefficient  $B$  responsible for a nonlinear small-scale dynamics.

We conclude that to provide an acceptable fit of the dLDN model prediction to the Lagrangian experimental data [18] *nonlinear* small-scale interactions encoded in the turbulent viscosity  $\nu_t$  are essential.

Sample fit of the dLDN probability density function  $P(a)$  given by Eq. (65) and contribution to the fourth-order moment,  $a^4 P(a)$ , are shown in Figs. 5 and 6, respectively. In the numerical fit, we have put, in accord to the redefinitions (52), the wave number parameter  $k = 1$  and the additive noise intensity parameter  $\alpha = 1$  in Eq. (65) and fitted the remaining three parameters  $\nu_0$ ,  $D$ , and  $B$ . One can observe a good agreement with the experimental data. Particularly, the dLDN contribution to the kurtosis  $a^4 P(a)$  plotted in Fig. 6 does peak at the same points as the experimental curve (positions of the peaks depend mainly on  $D$ ). The central part of the dLDN distribution shown in the bottom panel of Fig. 5 fits the experiment to a higher accuracy as compared with the log-normal model (22) but yet depart from that of the experimental curve. This departure can be attributed to the approximation of  $\delta$ -correlated multiplicative noise used in the dLDN model (see discussion in Sec. III above).

Having the general form of the dLDN distribution evaluated explicitly, Eq. (65), one can derive higher acceleration moments  $\langle a^n \rangle$ ,  $n = 2, 4, \dots$ . The associated integrals are not analytically tractable and can be evaluated numerically. We will consider these in Sec. IV below.

In the most general case ( $\lambda \neq 0$ ) the resulting  $P(a)$  is given due to an exponential of the exact integral (A3) which we do not represent here for brevity.

To sum up, we have made an important step forward with the dLDN model by having calculated  $P(a)$  exactly. We

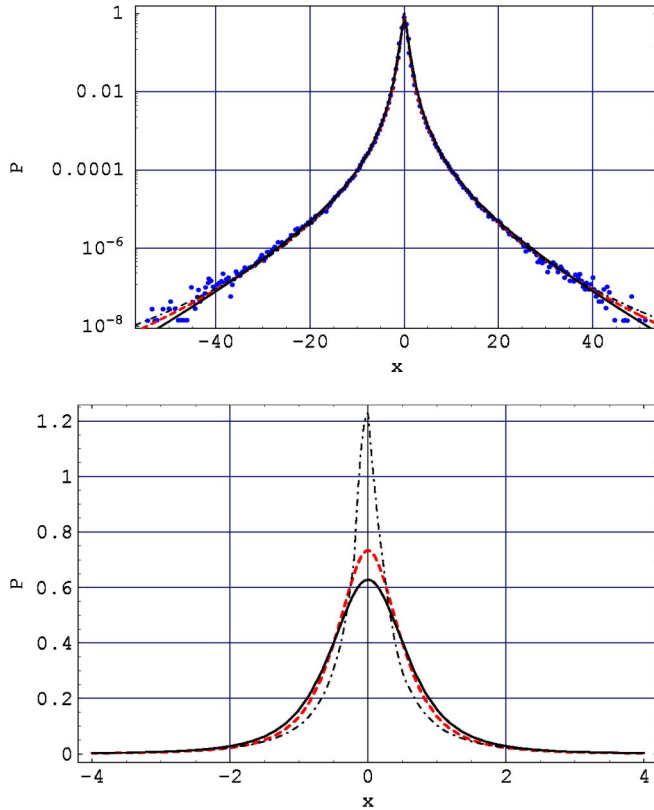


FIG. 5. Acceleration probability density function  $P(a)$ . Dots: experimental data at  $R_\lambda = 690$  by Crawford, Mordant, and Bodenschatz [18]. Dashed line: stretched exponential fit (13),  $b_1 = 0.513$ ,  $b_2 = 0.563$ ,  $b_3 = 1.600$ ,  $C = 0.733$ . Dot-dashed line: Beck log-normal model (22),  $s = 3.0$ . Solid line: Laval-Dubrulle-Nazarenko model (65),  $k = 1$ ,  $\alpha = 1$ ,  $D = 1.130$ ,  $B = 0.163$ ,  $\nu_0 = 2.631$ ,  $C = 1.805$ .  $x = a/\langle a^2 \rangle^{1/2}$  denotes normalized acceleration.

have shown that the dLDN model is capable to reproduce the recent Lagrangian experimental data on the acceleration statistics to a good accuracy. Particularly, we found that the predicted fourth-order moment density function does peak at the same value of acceleration,  $|a|/\langle a^2 \rangle^{1/2} \approx 10.2$ , as the experimental curve, in contrast to the predictions of the other considered stochastic models. The presence of the

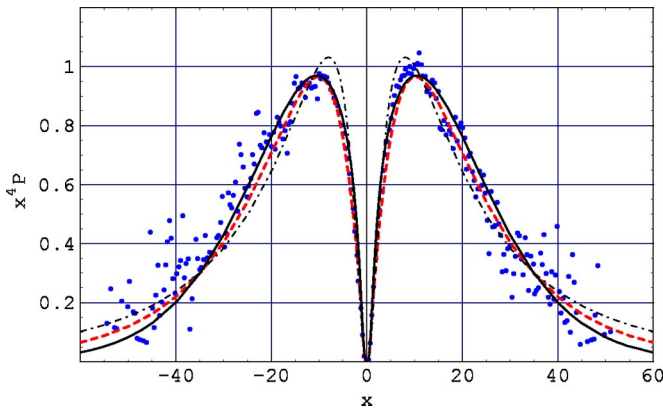


FIG. 6. Contribution to fourth-order moment  $a^4 P(a)$ . Notation is the same as in Fig. 5.

$\delta$ -correlated multiplicative noise and the nonlinearity (turbulent viscosity) in the model Langevin equation was found to be of much importance. The considered RIN models provide less but yet acceptable accuracy of the low-probability tails although they employ only one free parameter, which can be fixed by certain phenomenological arguments, as compared to the dLDN model, which contains four free parameters. However, we stress that in contrast to the LDN model the considered RIN models have a meager support from the turbulence dynamics.

#### IV. CONDITIONAL PROBABILITY DENSITY FUNCTION OF THE ACCELERATION

In the very recent paper [20] new experimental data on the conditional probability density function of the transverse acceleration,  $P(a|u)$ , have been reported. In general, this representation is in agreement with the proposed idea that velocity fluctuations  $u$  are directly involved in the stochastic acceleration dynamics [12] represented in Sec. II A 3.

Also, the observed conditional acceleration component variance has been found to be in a good agreement with the Sawford *et al.* scaling relation (see Ref. [20] and references therein)

$$\langle a^2|u \rangle \sim u^6, \quad (66)$$

obtained to a leading order in the same component  $u$  (not to be confused with the rms velocity  $\bar{u} = \langle u^2 \rangle^{1/2}$ ).

The experimental data reveal highly non-Gaussian, stretched exponential character of  $P(a|u)$ , very similar to that of  $P(a)$ , for fixed  $u$  ranging from zero up to three rms velocity  $\bar{u}$  [20] as opposed to the theoretical result that  $P(a|u)$  is a Gaussian in  $a$  due to the simple RIN model (6), with arbitrary  $\beta = \beta(u)$ , or due to the more general RIN model (33). Similarity between the experimental  $P(a|u)$  and  $P(a)$  suggests that they share the process underlying the fluctuations. Below, we address this important problem within the framework of the RIN approach.

The idea is that the stretched exponential form of the tails of the observed conditional distribution  $P(a|u)$  could be assigned solely to small time scales, while the marginal probability distribution  $P(a)$  is developed from  $P(a|u)$  at large time scales, in accord to the two-time-scale dynamics.

This requires some modification in the simple RIN models. The sole use of the  $\delta$ -correlated Gaussian-white additive noise, with fluctuating intensity depending on  $u$ , and a linear force  $F(a) = -a$ , with fluctuating  $\gamma = \gamma(u)$ , is not capable to explain the stretching in the observed  $P(a|u)$ , as it implies only Gaussian conditional probability density function  $P(a|u)$ , for any fixed  $u$ .

However, it is known that accounting for the *multiplicative*  $\delta$ -correlated Gaussian-white noise in the drift term of Langevin equation implies stretched exponential tails.

Hence we can simply follow the dLDN ansatz as a constitutive model (see Sec. II C) using the assumption that the

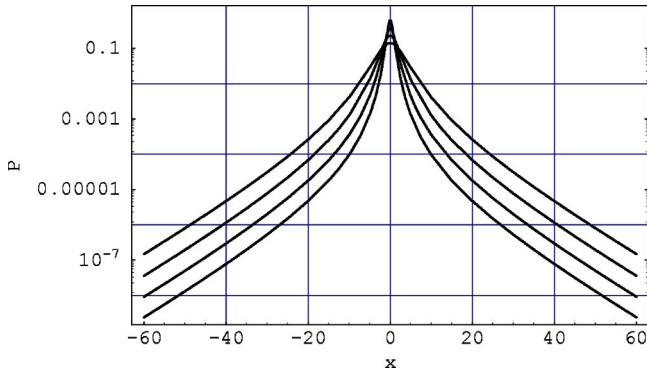


FIG. 7. Conditional probability density function  $P(a|u)$  given by Eq. (65) for  $\alpha = e^u$ ,  $k = 1$ ,  $D = 1.130$ ,  $B = 0.163$ ,  $\nu_0 = 2.631$ . The inner curve:  $u = 0$ . The outer curve:  $u = 3$ .  $x = a/\langle a^2 \rangle^{1/2}$  denotes normalized acceleration.

additive noise intensity  $\alpha$  appearing in the stationary probability distribution  $P(a|D, \alpha, B, \nu_0)$  given by Eq. (65) depends on  $u$ .

Here, we put the parameter  $\lambda$  measuring coupling of the noises to each other to zero ignoring thus the skewness effect, which is very small for both the experimental  $P(a|u)$  and  $P(a)$  [17,20]. This effect is nevertheless of much interest since it is associated with the relationship between stretching and vorticity in a three-dimensional flow. More important here is that it may imply additional stretching of the tails as well [see  $\lambda$  dependent terms in Eq. (A3)]. This possible way to explain stretched exponential tails of the observed  $P(a|u)$  can be considered elsewhere.

Following the arguments and techniques presented in Sec. II A 3, the marginal probability distribution  $P(a) = P(a|D, B, \nu_0)$  is obtained by integrating out  $u$  in

$$P(a|u) = P(a|D, \alpha(u), B, \nu_0), \quad (67)$$

with an appropriate choice of the function  $\alpha(u)$ , for example,  $\alpha(u) = e^u$ , and some probability distribution of  $u$ , for example, a Gaussian one with zero mean. Note that once  $P(a|D, \alpha(u), B, \nu_0)$  is fitted to the experimental curves of the conditional  $P(a|u)$  there formally remains only one parameter to be fitted in the marginal  $P(a)$ , the variance of the Gaussian distribution of  $u$ , i.e., the rms velocity  $\bar{u}$ .

The normalized conditional distribution (67) given by Eq. (65) with  $\alpha = e^u$  is shown in Fig. 7, for four values  $u = 0, 1, 2, 3$ , and the other parameters fixed. One can observe an increase of the variance with the increase of  $u$  and a good qualitative agreement with the experimental curves  $P(a|u)$  [20]. We note that the velocity fluctuations are present only in the definition of the LDN additive noise (45) which can be viewed as a hint that only additive noise intensity essentially depends on  $u$ . These results give an independent support to the model represented in Sec. II A 3.

We have checked a different reasonable assumption that the multiplicative noise intensity parameter  $D$  depends on the velocity fluctuations  $D \approx e^u$  with the other parameters fixed. The result is shown in Fig. 8. One can observe that the change of the shape of  $P(a|u)$  defined as

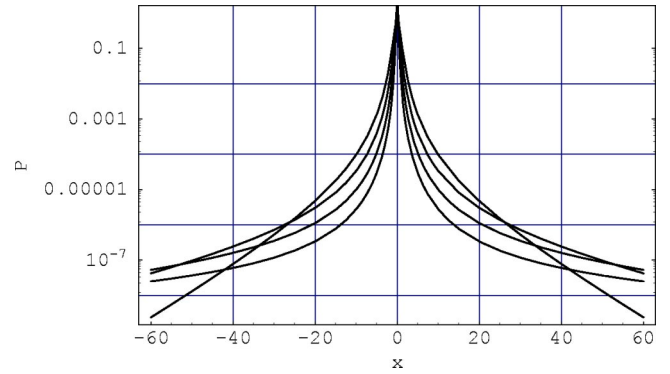


FIG. 8. Conditional probability density function  $P(a|u)$  given by Eq. (65) for  $\alpha = 1$ ,  $k = 1$ ,  $D = 1.13e^u$ ,  $B = 0.163$ ,  $\nu_0 = 2.631$ . The outer curve:  $u = 0$ . The inner curve:  $u = 3$ .  $x = a/\langle a^2 \rangle^{1/2}$ .

$P(a|D(u), \alpha, B, \nu_0)$  with the increase of  $u$  does not qualitatively meet that observed in the experiments [20]. We note that an increase of  $D$ , i.e., stronger multiplicative noise, is generally understood as the pronounced increase of the relative chance for a fluid particle to have higher accelerations as compared to low accelerations, due to the multiplicative random process. This point of view is confirmed by Fig. 8. Also, for a completeness in Fig. 9 we represent sample dependencies of  $P(a|D, \alpha, B, \nu_0)$  on the parameters  $B$  and  $\nu_0$ .

Using the dLDN probability function  $P(a|D, \alpha(u), B, \nu_0)$  one can compute  $\langle a^2|u \rangle$  and compare the result with the

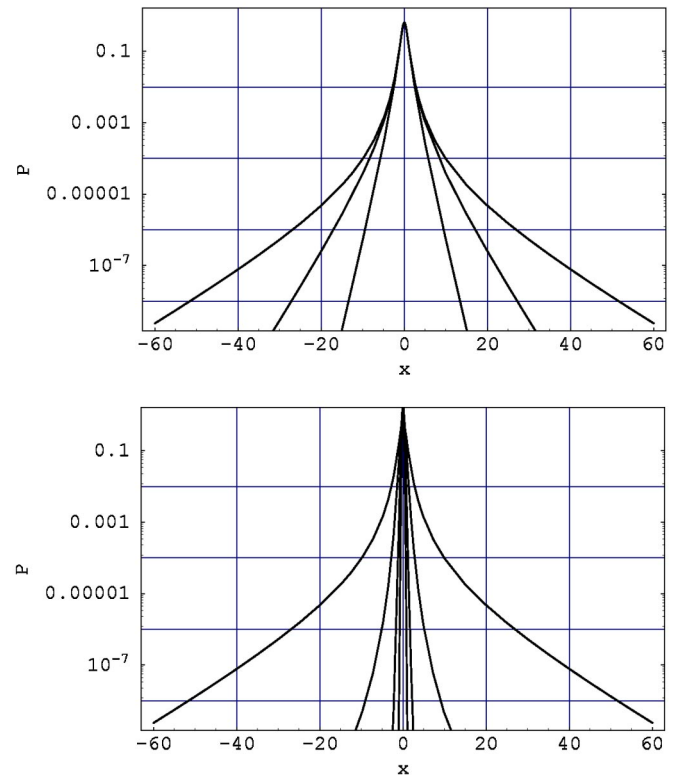


FIG. 9. Conditional probability density function  $P(a|u)$  given by Eq. (65). Top panel:  $\alpha = 1$ ,  $k = 1$ ,  $D = 1.130$ ,  $B = 0.163e^u$ ,  $\nu_0 = 2.631$  (the outer curve,  $u = 0$ ; the inner curve,  $u = 2$ ). Bottom panel:  $\alpha = 1$ ,  $k = 1$ ,  $D = 1.130$ ,  $B = 0.163$ ,  $\nu_0 = 2.631e^u$  (the outer curve,  $u = 0$ ; the inner curve,  $u = 3$ ).  $x = a/\langle a^2 \rangle^{1/2}$ .

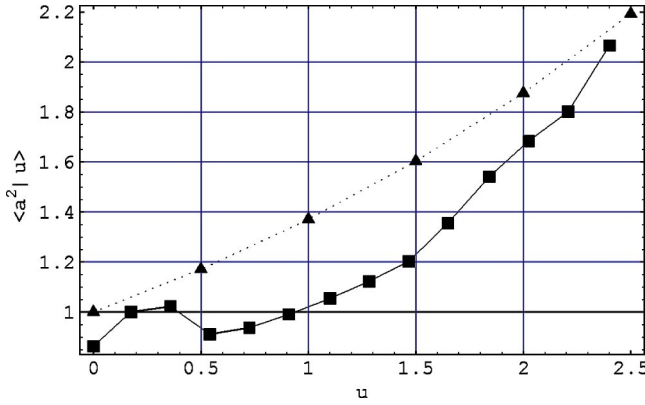


FIG. 10. The normalized conditional acceleration variance  $\langle a^2 | u \rangle$  as a function of normalized velocity fluctuations  $u / \langle u \rangle^{1/2}$ . Boxes: the experimental data on  $\langle a^2 | u \rangle / \langle a^2 \rangle$  [20], triangles:  $\langle a^2 | u \rangle / \langle a^2 | 0 \rangle$  with  $P(a|u)$  given by Eq. (65) for  $\alpha = e^{u/3}$ ,  $k = 1$ ,  $D = 1.130$ ,  $B = 0.163$ , and  $\nu_0 = 2.631$ .

predicted scaling relation (66) and the experimental data [20]. A sample plot of  $\langle a^2 | u \rangle$  is shown in Fig. 10, where we have used the exponential in the form  $\alpha = e^{u/u_0}$  to provide possibility for a fitting to the experimental data (boxes). Although with the fitted exponent,  $u_0 = 3$ , the result (triangles) exhibits a departure to the experiment; qualitatively the model implies a correct behavior of the conditional acceleration variance.

To summarize, the observed stretched exponential form of the conditional acceleration probability density function  $P(a|u)$  can be understood within the framework of the dLDN model (65) due to the effect of the multiplicative noise under the assumption that the additive noise intensity  $\alpha$  depends on velocity fluctuations  $u$ . The alternative assumption that the multiplicative noise intensity depends on  $u$  seems not to be in a qualitative agreement with the shapes of experimental curves at the different values of  $u$  except for  $u = 0$ . The predicted conditional acceleration variance  $\langle a^2 | u \rangle$  with  $\alpha = e^{u/u_0}$ ,  $u_0 = 3$ , have been found in a good qualitative agreement with the experimental curve. However, we observe a departure to the experimental data.

## V. DISCUSSION

We conclude with a few remarks.

(i) It is interesting to note that a universal probability density function  $f(u)$  could be identified with the help of the relation

$$\int_{-\infty}^{\infty} du u^6 f(u) \sim \bar{u}^{9/2}, \quad (68)$$

stemming from a comparison of the Heisenberg-Yaglom scaling relation (29) and the scaling (66), both recently confirmed by the experiments, where we assume that  $\int_{-\infty}^{\infty} du \langle a^2 | u \rangle f(u) \sim \langle a^2 \rangle$ . Obviously, the choice of a normalized Gaussian probability density function with zero mean for  $f(u)$  does not lead to the above relation since it

implies  $\sim \bar{u}^6$ . This can be viewed as a signal for selecting a different probability distribution of  $u$ , such as that of a stretched exponential form.

(ii) In the present paper, we put the parameter  $\lambda$ , which measures the coupling between the multiplicative and additive noises in the dLDN model, to zero discarding thus skewness effects in the predicted  $P(a|u)$  and  $P(a)$ . This effect is of much interest to study in order to estimate  $\lambda$  using the fitting to Lagrangian experimental data on the longitudinal component of acceleration with respect to the trajectory ( $\lambda = 0$  by definition for the transverse component of acceleration). Presumably it is small due to small skewness of both the observed  $P(a|u)$  and  $P(a)$  for the measured  $x$  component of acceleration [18].

(iii) Following the RIN approach presented in this paper it is of interest to evaluate the proposed averaging of the dLDN probability distribution  $P(a|D, \alpha(u), B, \nu_0)$  given by Eq. (65) over normally distributed  $u$  with  $\alpha$  taken to be  $\alpha = e^u$ . This is equivalent to the averaging over log normally distributed  $\alpha$ . A comparison of the resulting distribution with the Lagrangian experimental data can be made elsewhere.

(iv) In the present paper we have not reviewed a recent work by Reynolds [9]. A comparison of the results of the Reynolds model with that of the stochastic models proposed in Refs. [5,6] can be found in the recent paper by Mordant *et al.* [20].

## APPENDIX: EXACT INTEGRALS

Exact indefinite integrals, up to a constant term which does not depend on  $a$ , used in calculating the definite integral entering the probability density function (48) are given below.

At  $\nu_t = \nu_0$ ,

$$\begin{aligned} & \int da \frac{-\nu_0 k^2 a - Da + \lambda}{Da^2 - 2\lambda a + \alpha} \\ &= -\frac{D + \nu_0 k^2}{2D} \ln[Da^2 - 2\lambda a + \alpha] \\ &+ \frac{\lambda \nu_0 k^2}{D \sqrt{D\alpha - \lambda^2}} \arctan \frac{Da - \lambda}{\sqrt{D\alpha - \lambda^2}}. \quad (A1) \end{aligned}$$

At  $\nu_t = B|a|/k$ , for positive and negative  $a$ , respectively,

$$\begin{aligned} & \int da \frac{\mp Bka^2 - Da + \lambda}{Da^2 - 2\lambda a + \alpha} \\ &= \mp \frac{Bka}{D} - \frac{D^2 \pm 2B\lambda k}{2D^2} \ln[Da^2 - 2\lambda a + \alpha] \\ &\pm \frac{B(D\alpha - 2\lambda^2)k}{D^2 \sqrt{D\alpha - \lambda^2}} \arctan \frac{Da - \lambda}{\sqrt{D\alpha - \lambda^2}}. \quad (A2) \end{aligned}$$

In the general case, we have obtained a cumbersome expression



$$\begin{aligned}
& \int da \frac{-\nu_t k^2 a - Da + \lambda}{Da^2 - 2\lambda a + \alpha} \\
&= -\frac{\nu_t k^2}{D} - \frac{1}{2} \ln[Da^2 - 2\lambda a + \alpha] \\
&\quad - \frac{2B\lambda k}{D^2} \ln[2Bka + \nu_t k^2] + F(c) + F(-c),
\end{aligned} \tag{A3}$$

where we have denoted

$$\begin{aligned}
F(c) = \frac{c_1 k^2}{2c_2 D^2 c} \ln \left\{ \frac{2D^3}{c_1 c_2 (c - Da + \lambda)} [B^2(\lambda^2 + c\lambda - D\alpha)a \right. \\
\left. + c(D\nu_t^2 k^2 + c_2 \nu_t)] \right\}, \tag{A4}
\end{aligned}$$

$$c = -i\sqrt{D\alpha - \lambda^2}, \quad \nu_t = \sqrt{\nu_0^2 + B^2 a^2 / k^2}, \tag{A5}$$

$$c_1 = B^2(4\lambda^3 + 4c\lambda^2 - 3D\alpha\lambda - cD\alpha) + D^2(c + \lambda)\nu_0^2 k^2, \tag{A6}$$

$$c_2 = \sqrt{B^2(2\lambda^2 + 2c\lambda - D\alpha)k^2 + D^2\nu_0^2 k^4}. \tag{A7}$$

Some useful formulas used in verifying the limits  $B \rightarrow 0$  and  $D \rightarrow 0$  are

$$\arctan x = \frac{i}{2} [\ln(1 - ix) - \ln(1 + ix)], \tag{A8}$$

$$\lim_{D \rightarrow 0} \frac{1}{D} \ln[1 + Da^2] = a^2. \tag{A9}$$

- 
- [1] C. Tsallis, *J. Stat. Phys.* **52**, 479 (1988).  
[2] R. Johal, e-print cond-mat/9909389.  
[3] A.K. Aringazin and M.I. Mazhitov, *Physica A* **325**, 409 (2003); e-print cond-mat/0204359.  
[4] C. Beck and E.G.D. Cohen, *Physica A* **322**, 267 (2003); e-print cond-mat/0205097.  
[5] C. Beck, e-print cond-mat/0212566.  
[6] C. Beck, *Phys. Rev. Lett.* **87**, 180601 (2001); e-print cond-mat/0110073.  
[7] G. Wilk and Z. Wlodarczyk, *Phys. Rev. Lett.* **84**, 2770 (2000).  
[8] C. Beck, *Physica A* **277**, 115 (2000); *Phys. Lett. A* **287**, 240 (2001); *Europhys. Lett.* **57**, 329 (2002); e-print cond-mat/0105371.  
[9] A.M. Reynolds, *Phys. Fluids* **15**, L1 (2003).  
[10] A.K. Aringazin and M.I. Mazhitov, e-print cond-mat/0212462.  
[11] A.K. Aringazin and M.I. Mazhitov, e-print cond-mat/0301040.  
[12] A.K. Aringazin and M.I. Mazhitov, *Phys. Lett. A* **313**, 284 (2003); e-print cond-mat/0301245.  
[13] T. Gotoh and R.H. Kraichnan, e-print nlin.CD/0305040.  
[14] B. Castaing, Y. Gagne, and E.J. Hopfinger, *Physica D* **46**, 177 (1990).  
[15] B.L. Sawford, *Phys. Fluids A* **3**, 1577 (1991); S.B. Pope, *Phys. Fluids* **14**, 2360 (2002).  
[16] A.N. Kolmogorov, *J. Fluid Mech.* **13**, 82 (1962); L.D. Landau and E. M. Lifschitz, *Fluid Mechanics*, 2nd ed. (Pergamon Press, Oxford, 1987).  
[17] A. La Porta, G.A. Voth, A.M. Crawford, J. Alexander, and E. Bodenschatz, *Nature (London)* **409**, 1017 (2001); G.A. Voth, A. La Porta, A.M. Crawford, E. Bodenschatz, and J. Alexander, *J. Fluid Mech.* **469**, 121 (2002); e-print physics/0110027.  
[18] A.M. Crawford, N. Mordant, E. Bodenschatz, and A.M. Reynolds, *Phys. Rev. Lett.* (to be published), e-print physics/0212080.  
[19] N. Mordant, J. Delour, E. Leveque, A. Arneodo, and J.-F. Pinton, *Phys. Rev. Lett.* **89**, 254502 (2002); e-print physics/0206013.  
[20] N. Mordant, A.M. Crawford, and E. Bodenschatz, *Physica D* (to be published) e-print physics/0303003.  
[21] R.H. Kraichnan and T. Gotoh, data presented at the CNLS Workshop on Anomalous Distributions, Nonlinear Dynamics, and Nonextensivity, Santa Fe, NM, 2002.  
[22] B. Hnat, S.C. Chapman, and G. Rowlands, *Phys. Rev. E* **67**, 056404 (2003).  
[23] J.-P. Laval, B. Dubrulle, and S. Nazarenko, *Phys. Fluids* **13**, 1995 (2001); e-print physics/0101036.  
[24] J.-P. Laval, B. Dubrulle, and J.C. McWilliams, *Phys. Fluids* **15**, 1327 (2003).  
[25] J.F. Muzy and E. Bacry, *Phys. Rev. E* **66**, 056121 (2002).  
[26] N. Mordant, P. Metz, O. Michel, and J.-F. Pinton, physics/0103084; *Phys. Rev. Lett.* **87**, 214501 (2001).  
[27] Ch. Renner, J. Peinke, and R. Friedrich, e-print physics/0211121; Ch. Renner, J. Peinke, R. Friedrich, O. Chantal, and B. Chabaud, *Phys. Rev. Lett.* **89**, 124502 (2002).  
[28] S.C. Chapman, G. Rowlands, and N.W. Watkins, e-print cond-mat/0302624.  
[29] B. Portelli, P.C.W. Holdsworth, and J.-F. Pinton, *Phys. Rev. Lett.* **90**, 104501 (2003).  
[30] S. Nazarenko, N.K.-R. Kevlahan, and B. Dubrulle, *Physica D* **139**, 158 (2000).  
[31] H. Nakao, *Phys. Rev. E* **58**, 1591 (1998).  
[32] Y. Kuramoto and H. Nakao, *Phys. Rev. Lett.* **76**, 4352 (1996); **78**, 4039 (1997).